PROGRESSIVE DAMAGE STUDY OF NCF COMPOSITES UNDER COMPRESSIVE LOADING

L. M. Ferreira[a*], E. Graciani[a], F. París[a]

[a] *Grupo de Elasticidad y Resistencia de Materiales, Escuela Técnica Superior de Ingenieros, Universidad de Sevilla, Camino de los Descubrimientos s/n 41092 Sevilla, España.*
**luismmferreira@ipt.pt*

Keywords: Non-crimp fabric, FE model, Progressive damage.

Abstract

A mesoscopic scale 3D finite element (FE) model of the representative unit cell of a $[0,90]_n$ non-crimp fabric laminate is used to study the progressive damage under compressive loading. The tows of the unit cell have been generated with a straight FE mesh, the waviness of the fibres having been taken into account with the definition of the mechanical properties of each element according to the actual direction of the fibres. The maximum strain criterion has been employed in the numerical study of the progressive damage to determine the onset of the material damage under the compressive loading. The numerical predictions are discussed and compared both with previous numerical studies in which the tows had been defined with non-linear behaviour and with experimental data.

1. Introduction

The use of non-crimp fabric (NCF) composites has been significantly increasing in the past decade due to their cost-performance benefits. As the woven-fabric composites, the NCF composites are made from dry preforms. Since they produced in a continuous process, by laying groups of fibre tows (or tows for short), at a specific orientation, sequentially on a conveyor system and held in position by a stitching yarn, they create, in theory, a fabric without fibre waviness. In practice, however, NCF composites present a complex mesoscopic 3D structure with tows in different orientations, stitching yarns, fibre crimp and resin rich areas.

Several FE models of NCF composites have been generated to evaluate their mechanical performance prior to experimental characterization [1-4]. However, generating efficient FE models capable of reproducing the complexity of their structure and also capable of modelling damage is still a challenge.

The work presented in this paper, is dedicated to the study of the progressive damage of NCF composites under compressive loading, using 3D FE models of the representative unit cell (RUC) of a $[0,90]_n$ NCF laminate with fibre crimped tows. Since, at this level, tows can be considered identical to unidirectional laminates, one typical failure criterion commonly used for unidirectional laminates, the maximum strain failure criterion, has been chosen has onset to determine the failure initiation.

2. Mesoscopic approach of the NCF laminate

2.1. Numerical models

A mesoscopic scale 3D FE model of the RUC of a $[0,90]_n$ NCF laminate, with fibre crimp due to nesting of the tows, has been generated using structural solid element SOLID185 from ANSYS® FE code [5]. The unit cell employed is composed by 4 laminas (0º, 90º, 0º, 90º) and each lamina contains two half tows and a resin pocket between them, see Fig. 1(a) and Fig. 1(b). To clarify the out-of-plane fibre crimp of the tows, an equivalent unit cell with the fibre crimp modelled according to the classical modelling approach is represented in Fig. 1(c) and Fig. 1(d). Notice that the resin has been removed to better understand the tows shape and orientation.

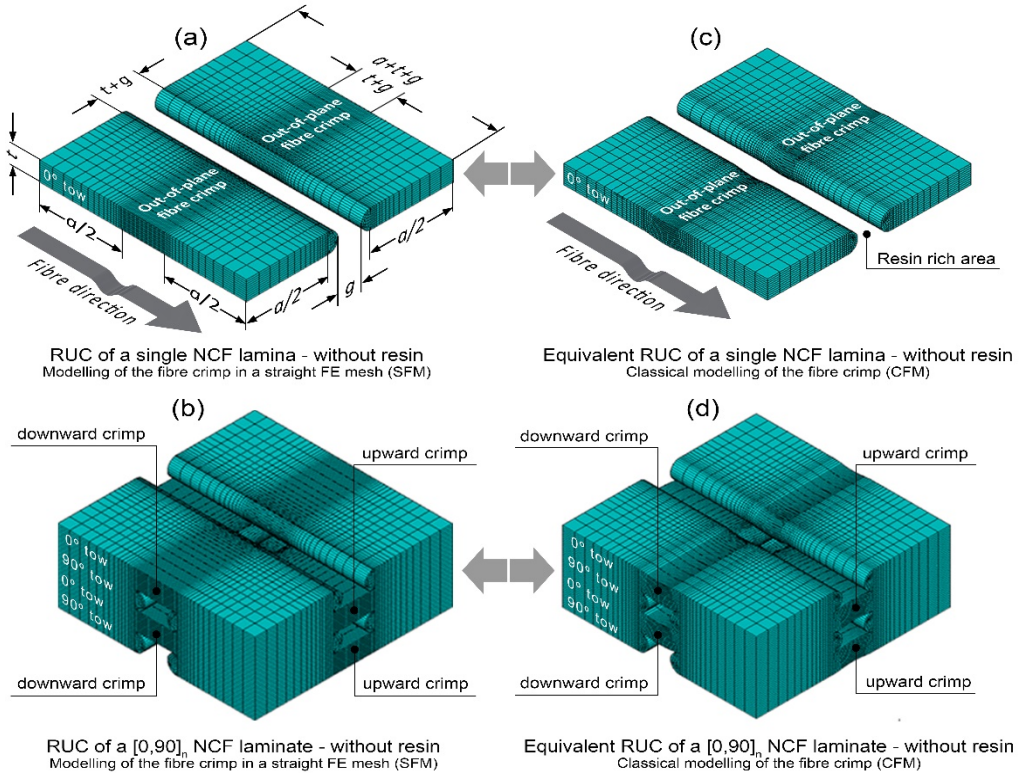

Fig. 1. 3D FE model of the representative unit cell without resin. (a) Single NCF lamina – SFM, (b) $[0,90]_n$ NCF laminate – SFM, (c) Single NCF lamina – CFM, (d) $[0,90]_n$ NCF laminate – CFM.

The curvature of the tows represented in Fig. 1(a) and Fig. 1(b) has been omitted in the geometry of the model, although taking into consideration the waviness of the fibres, following the modelling approach presented in [3]. This approach allows a straight FE mesh to be used.

A maximum fibre crimp angle of 12º has been chosen for this study based on the fact that previous results showed, for the material studied, a satisfactory agreement between the apparent in-plane stiffness properties and the experimental evidence for angles in a range of 9º to 12º [6, 7].

The geometrical parameters employed are shown in Fig. 1(a), where *a* represents the length of the tow not affected by the fibre crimp, *t* the thickness of each lamina and *g* the width of the gap left between two adjacent tows of each lamina. The values of these parameters have been estimated from the results of the microstructure characterization measured in [8] having taken,

$a = 2.06$ mm, $t = 0.24$ mm and $g = 0.30$ mm. These parameters and the maximum fibre crimp angle get the same value in all tows involved. An average fibre volume fraction of each lamina of $V_f^l = 60\%$ has been obtained from the observed average fibre volume fraction of the tows $V_f^t = 69\%$ [9], and from the relative dimensions of the cross-sections of the tow and of the lamina.

Taking advantage of the symmetry of the problem, only one quarter of the RUC has been employed in this study, see Fig. 2. In accordance with the global coordinate system *xyz*, the plane of the laminate is the *xy*-plane and *z* is the through-thickness direction. The local coordinate system 123 corresponds to the actual direction of the fibres (direction 1, Fig. 2).

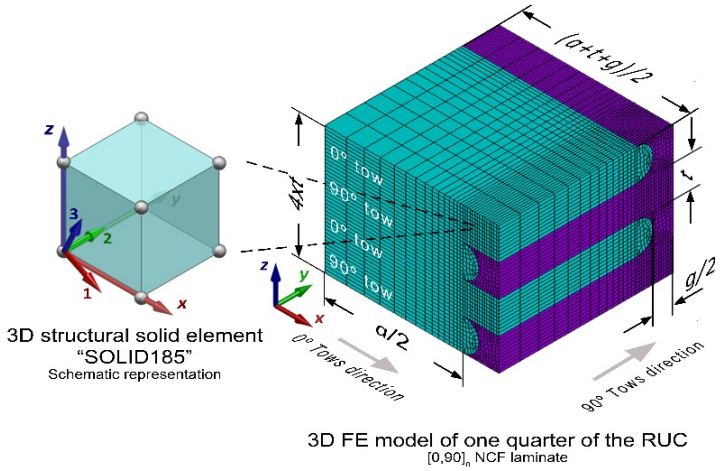

Fig. 2. 3D FE model and dimensions of a quarter of the $[0,90]_n$ NCF laminate developed.

2.2. Mechanical properties of the constituents

In order to be able to carry out the progressive damage analysis with ANSYS® [5], the tows and resin must be defined with linear elastic behaviour.

At the mesoscopic scale, the stiffness properties required in order to carry out the FE analysis are those of the resin pockets and of the tows. Since the tows are constituted by a large number of parallel fibres uniformly distributed and impregnated by a resin, their behaviour can be considered transversely isotropic (with elastic constants: E_{11}^t, ν_{12}^t, G_{12}^t, E_{22}^t, ν_{23}^t and G_{23}^t).

The FE model has been generated according to the NCF composites tested within the FALCOM project [10-12]. However, as no experimental measurements were performed to estimate the stiffness properties of the tows, the rule of mixtures has been employed as an averaging technique to estimate their values as a function of the elastic properties of the fibre and of the resin, see Table 1.

V_f^t	E_{11}^t (GPa)	E_{22}^t (GPa)	ν_{12}^t	ν_{23}^t	G_{12}^t (GPa)	G_{23}^t (GPa)
60%	165.5	11.43	0.30	0.42	4.03	4.03

Table 1. Stiffness properties of the tows obtained with the rule of mixtures.

The resin employed is characterized by an elastic modulus $E^m = 3.50$ GPa , a Poisson's ratio $\nu^m = 0.42$ and a corresponding shear modulus $G^m = 1.23$ GPa. Carbon fibres, being a transversely isotropic material, exhibit the following relations: $E_{22}^f = E_{33}^f$, $\nu_{12}^f = \nu_{13}^f$, $G_{12}^f = G_{13}^f$. According to the rule of mixtures, the values of the elastic constants in the planes transverse to the fibre axis, E_{22}^f, ν_{23}^f and G_{23}^f, are not needed to estimate the apparent stiffness properties of the tows neither in the longitudinal plane nor in the transverse planes. In this way, the carbon fibre has been characterized by a longitudinal elastic modulus $E_{11}^f = 237$ GPa , a Poisson's ratio $\nu_{12}^f = 0.25$ and a shear modulus $G_{12}^f = 94.8$ GPa.

2.3. Boundary conditions

The boundary conditions applied to the faces of the FE model serve to impose a compressive stress state and to guarantee the displacements compatibility in the limits of the model with the rest of the structure. Symmetry conditions have been assumed in the faces parallel to the *xz*-plane and in one of the faces parallel to *yz*-plane, while in the opposite face, parallel to the *yz*-plane, a constant displacement *(k)* in the compression load direction has been applied to all nodes, and to ensure that they all displace the same, all nodes have been coupled. In this way, the compression load is given by the sum of the reaction forces of all nodes at $x = 0$. The boundary conditions in the top and bottom faces (parallel to the *xy*-plane) must guarantee the compatibility of the unit cell under consideration with the adjacent unit cells. Thus, the displacements of the nodes in both faces are coupled to ensure that the extension in the through-thickness direction is constant through the whole model. Notice that with the boundary conditions employed, the NCF laminate has an infinite length along the *y*-axis.

3. Progressive damage study

3.1. Damage initiation criteria and damage evolution law

Progressive damage studies with ANSYS® [5] requires a damage initiation criteria and a damage evolution law to be completed. For this paper, the maximum strain criterion has been chosen to determine the onset of the material damage under the compressive loading for the tensile/compressive fibre failure mode and for the tensile/compressive matrix failure mode. The values employed for the tows have been obtained from a standard unidirectional carbon fibre composite with a fibre volume fraction of 60% [13].

Following the onset of damage, material stiffness reduction occurs immediately (material property degradation method). The amount of reduction is based on damage variables specified in the damage evolution law in which coefficient values are addressed to the tensile fibre stiffness reduction $\left(d_f^+\right)$, compressive fibre stiffness reduction $\left(d_f^-\right)$, tensile matrix stiffness reduction $\left(d_m^+\right)$ and compressive matrix stiffness reduction $\left(d_m^-\right)$. The allowable values of these coefficients are between 0 and 1, where 0 corresponds to no reduction in the material stiffness in the affected mode after damage initiation and 1 to a complete stiffness loss in the affected mode. In the present study, a value of 0.2 has been considered for all the damage variables.

The constitutive relationship for a damage orthotropic material is given by (1).

$$\sigma = \begin{bmatrix} \frac{C_{11}}{(1-d_f)} & C_{12} & C_{13} & 0 & 0 & 0 \\ C_{21} & \frac{C_{22}}{(1-d_m)} & C_{23} & 0 & 0 & 0 \\ C_{31} & C_{32} & \frac{C_{33}}{(1-d_m)} & 0 & 0 & 0 \\ 0 & 0 & 0 & \frac{C_{44}}{(1-d_s)} & 0 & 0 \\ 0 & 0 & 0 & 0 & \frac{C_{55}}{(1-d_s)} & 0 \\ 0 & 0 & 0 & 0 & 0 & \frac{C_{66}}{(1-d_s)} \end{bmatrix} \varepsilon \quad (1)$$

Where, C is the compliance matrix of the undamaged material, $\boldsymbol{\sigma}$ is the nominal Cauchy stress (effective stress averaged over both damaged and undamaged domains) and $\boldsymbol{\varepsilon}$ is the total elastic strain. The damage variables for calculating the elasticity matrix are determined by (2).

$$\begin{aligned} d_f &= \begin{cases} d_f^+, \ if \ \lambda_f^+ > 0 \\ d_f^-, \ if \ \lambda_f^- > 0 \end{cases} \\ d_m &= \begin{cases} d_m^+, \ if \ \lambda_m^+ > 0 \\ d_m^-, \ if \ \lambda_m^- > 0 \end{cases} \\ d_s &= 1-\left(1-d_f^+\right)\left(1-d_f^-\right)\left(1-d_m^+\right)\left(1-d_m^-\right) \end{aligned} \quad (2)$$

Where, d_s is the shear damage variable and $\lambda_f^+, \lambda_f^-, \lambda_m^+, \lambda_m^-$ are the fibre tension, fibre compression, matrix tension and matrix compression failure calculated from the effective stress measured in the undamaged domain.

3.2. Numerical results

The progressive damage sequence throughout the unit cell, from the load at which damage initiates (200 MPa) to the load at which the failure of the laminate is predicted (680 MPa), is shown in Fig. 3. Three damage status are represented; undamaged, partially damaged and completely damaged. The material is considered to be undamaged when none of the onsets defined in the failure criterion has been reached. When at least one of the four damage modes (fibre tension, fibre compression, matrix tension, and matrix compression) is initiated the material is considered to be damaged. If all the damage modes are initiated, the material is considered to be completely damaged.

According to the numerical results, damage initiates at approximately 200 MPa in the part where the 0º tows are affected by the out-of-plane fibre crimp (where packages of resin appear between each two 90º tows), in particular where the misorientation angle of the fibres is maximum, see Fig. 3(a). Given the boundary conditions, the load imposed and the presence of the fibre crimp, the 0º tows suffer an instability phenomenon causing localized shear strains γ_{13} and thus giving rise to this potential failure location [6].

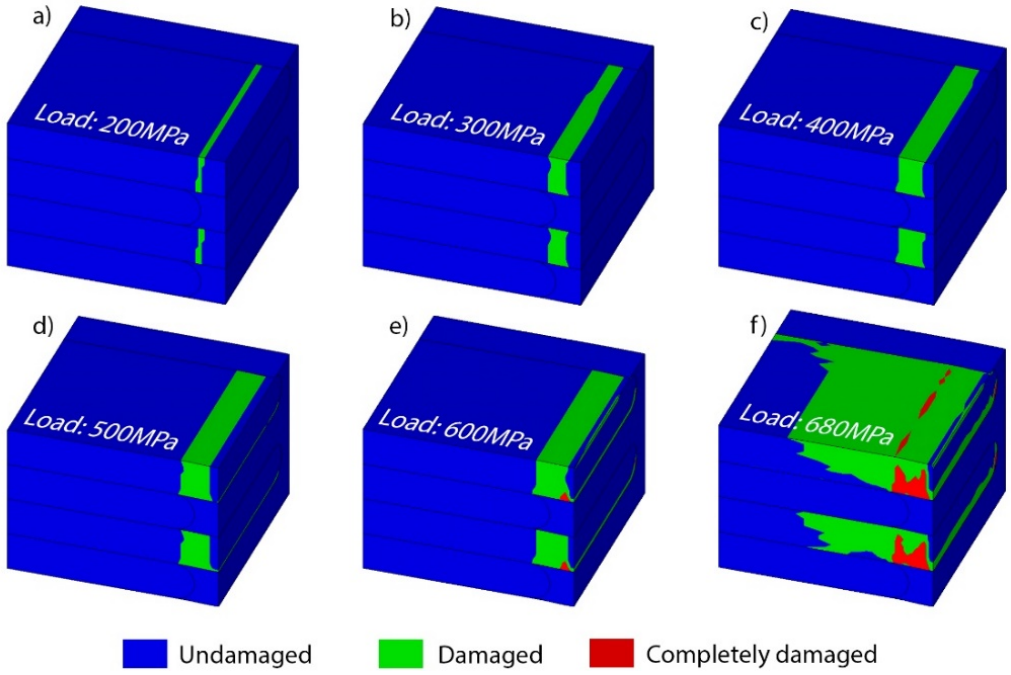

Fig. 3. Progressive damage sequence until failure of the NCF laminate is predicted.

When the compressive load increases up to 500 MPa, the damage propagates throughout the crimp location, causing the nonlinear response of the stress-strain curve with material property degradation *"MPD"*, see Fig. 4. Until this load step, the damage modes predicted are related to matrix tension and matrix compression, and according to equation (2) they are the only modes that contribute to the shear damage. Starting from 600MPa, completely damaged elements appear in the crimped location, see Fig. 3(e). This means that apart from the matrix damage, fibre damage has also been predicted. At 680 MPa, damage no longer is confined to the crimp location and it propagates throughout large part of the 0º tows, see Fig. 3(f). Moreover, it is possible to appreciate that the area of completely damaged elements increases in the crimp location. These events motivate the sudden loss of the NCF laminate stiffness and thus failure is predicted, see Fig. 4.

3.3. Comparison between numerical results and experimental data

The numerical compressive stress-strain curve obtained with the 3D FE model of the RUC of a $[0,90]_n$ NCF laminate with a 12º fibre crimp angle and with *MPD* has been compared in Fig. 4 with:

- A FE model without MPD, in which the tows have been modelled with linear shear behaviour in all planes. *"No MPD (linear)"*;
- A FE model without MPD, in which the tows have been modelled with nonlinear shear behaviour in the longitudinal and transverse through-thickness planes, 12-plane and 13-plane respectively. *"No MPD (nonlinear)";*
- Experimental data measured within the FALCOM project [14]. *"Experimental [FALCOM]"*.

In the FE model *"MPD (nonlinear)"*, the tows have been modelled with nonlinear shear behaviour in the longitudinal and transverse through-thickness planes, because in these planes the behaviour of the tows under shear loads is affected by the resin, whose behaviour is also nonlinear [1]. This nonlinearity in the mechanical behaviour of the tows has been introduced in

the FE model by a bilinear approximation of the shear stress-strain curve obtained by Ditcher [15]. The change of slope has been placed at a value $\left(\sigma_{12}^{*}\right)$ of 60 MPa of stress, see Table 2.

$\sigma_{12}^{*}\,(\mathrm{MPa})$	Slope I $G_{12}^{t,I}=G_{13}^{t,I}\,(\mathrm{GPa})$	Slope II $G_{12}^{t,II}=G_{13}^{t,II}\,(\mathrm{GPa})$
60	4.03	0.75

Table 2. σ_{12}^{*}, slope values I and II used to define the nonlinear shear behaviour of the tows.

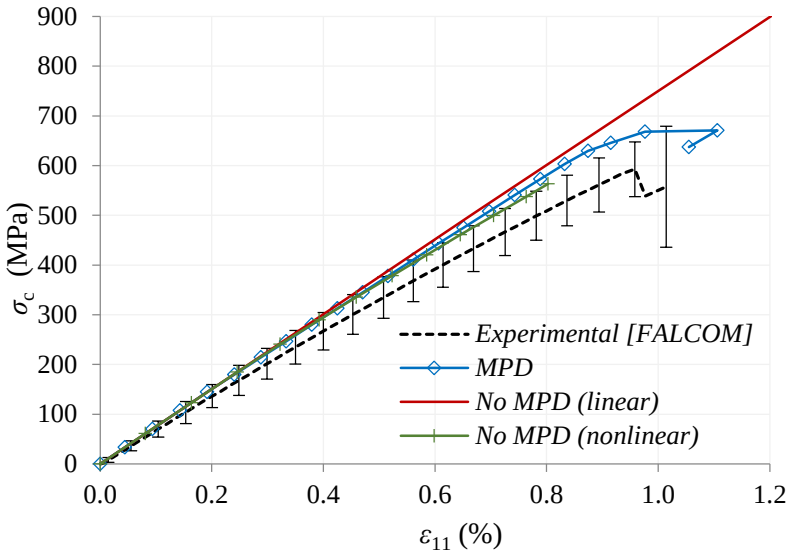

Fig. 4. Experimental and numerical **s**tress-strain curves.

A satisfactory agreement is found between experimental and numerical results if either the material property degradation *"MPD"* or the nonlinear shear behaviour of the tows *"No MPD (nonlinear)"* are taken into account in the FE model. On the other hand, it is clear that not considering any of these, which corresponds to the *"No MPD (linear)"* results, causes the solution to diverge from the remaining curves if higher compressive loads are considered. Until this moment, ANSYS® [5] only allows the progressive damage analysis to be performed if the undamaged material has a linear elastic behaviour. If it was possible to include, both the material property degradation and the nonlinear behaviour in the same FE model, the numerical results would have an even great agreement with the experimental data.

Regarding the failure prediction, a satisfactory agreement has also been found between the experimental and the numerical *"MPD"* results. However, the predicted failure depends on the damage initiation criteria and the damage evolution law considered. In both *"No MPD (nonlinear)"* and *"No MPD (linear)"* FE models, the load at which the solution stop to converge is not related with the prediction of failure of the laminate but with the fact that elements get highly distorted.

4. Conclusions

The progressive analysis of a $[0,90]_n$ NCF laminate under an in-plane compressive load has been studied using 3D FE models with fibre crimped tows. The maximum strain criterion has been employed to determine the onset of the material damage under the compressive loading.

The numerical results show that damage initiates in the part where the 0º tows are affected by the fibre crimp (in particular where the misorientation angle of the fibres is maximum) due to high localized shear strains γ_{13}. Completely damaged elements appear at approximately 600 MPa. When the load reaches 680 MPa, damage propagates throughout a large part of the 0º tows which motivates the sudden loss of the NCF laminate stiffness and thus failure load is predicted. Although, a satisfactory agreement has been found between the experimental and the numerical failure prediction, the predicted failure depends significantly on the damage initiation criteria and the damage evolution law considered in the study.

A satisfactory agreement is found between experimental and numerical results if either the material property degradation or the nonlinear shear behaviour of the tows are taken into account in the FE model. It is clear, that if it was possible to include, both the material property degradation and the nonlinear behaviour in the same FE model, the numerical results would have an even great agreement with the experimental data.

References

[1] Drapier S, Wisnom MR. Finite-element investigation of the compressive strength of non-crimp-fabric-based composites. *Compos Sci Technol.* 1999;59(8):1287-1297.
[2] Drapier S, Wisnom MR. A finite-element investigation of the interlaminar shear behaviour of non-crimp-fabric-based composites. *Compos Sci Technol.* 1999;59(16):2351-2362.
[3] Ferreira LM, Graciani E, París F. Modelling the waviness of the fibres in non-crimp fabric composites using 3D finite element models with straight tows. *Composite Structures.* 2014;107(0):79-87.
[4] Joffe R, Mattsson D, Modniks J, Varna J. Compressive failure analysis of non-crimp fabric composites with large out-of-plane misalignment of fiber bundles. *Compos Part a-Appl S.* 2005;36(8):1030-1046.
[5] ANSYS. Release 15. Swanson Analysis Systems Inc 2014.
[6] Ferreira LM. Study of the behaviour of non-crimp fabric laminates by 3D finite element models. PhD. Thesis. University of Seville, 2012.
[7] González A, Graciani E, París F. Prediction of in-plane stiffness properties of non-crimp fabric laminates by means of 3D finite element analysis. *Compos Sci Technol.* 2008;68(1):121-131.
[8] Mattsson D, Joffe R, Varna J. Characterisation of processability and manufacturing. Characterisation of microstructure. FALCOM/WP2:D2.1-4/LTU., 2004.
[9] Asp LE, Öhgren I, Holmberg JA. Determination of fibre content on RFI plates for G1c and OHT testing. FALCOM/WP3/SI/TECH001. 2004.
[10] Joffe R. Characterization of performance. Performance in tension. Elastic properties and failure. FALCOM/WP3:T3.2.1/LTU. 2004.
[11] Joffe R. Performance of non-crimp fabric composites in shear. *Key Eng Mater*. 2010;425:45-59.
[12] Mattsson D, Joffe R, Varna J. Damage in NCF composites under tension: Effect of layer stacking sequence. *Eng Fract Mech.* 2008;75(9):2666-2682.
[13] Composite Materials Handbook: Department of Defense of the United States of America; 1998.
[14] Sinclar R, Robinson P, Iannucci L. Directed compression tests on FALCOM biaxial cross-ply material. FALCOM/WP3/ICL/TR01. Imperial College London; 2005.
[15] Ditcher AK. The non-linear stress-strain behaviour of carbon fibre reinforced plastic and its effects on the analysis of laminated plates and sandwich beams. University of Bristol, Department of Aerospace Engineering, 1981.